THE UNIVERSITY OF MANITOBA

A SAMPLING SYSTEM FOR LOW FREQUENCY DIELECTRIC SPECTROSCOPY

by

WITOLD STANISLAW MATULEWICZ

A THESIS

SUBMITTED TO THE FACULTY OF GRADUATE STUDIES

IN PARTIAL FULFILMENT OF THE REQUIREMENTS FOR THE DEGREE

OF MASTER OF SCIENCE

DEPARTMENT OF AGRICULTURAL ENGINEERING

WINNIPEG, MANITOBA

October 1975

"A SAMPLING SYSTEM FOR LOW FREQUENCY

DIELECTRIC SPECTROSCOPY"

by

WITOLD STANISLAW MATULEWICZ

A dissertation submitted to the Faculty of Graduate Studies of the University of Manitoba in partial fulfillment of the requirements of the degree of

MASTER OF SCIENCE

ABSTRACT

A novel technique is described for fast permittivity measurement over the frequency range 0.5 Hz to 16 kHz.

A sampling system has been developed, to perform measurement of the current-time response to a voltage step of a capacitor containing a dielectric material.

The data is recorded at sixteen logarithmically spaced times with the base of 2 from 10 μs to 327.68 ms. Analog to digital conversion technique has been employed, in order to facilitate time to frequency domain transformation by means of digital computer. A computer program based on an appropriate Fourier transform has been developed for processing of the experimental data. The results of the relative permittivity and loss factor can be calculated at sixteen descrete frequencies spaced at octave intervals.

Particular emphasis is given to the problems concerning sampling circuitry.

ACKNOWLEDGMENTS

I wish to express my appreciation to Dr. S.S.Stuchly for suggesting this thesis subject and for his supervision through the entire work.

Sincere thanks are given to Dr. M.A.K.Hamid and Professor A.Jakobschuk for their critical comments.

Special thanks are due to Dr. G.E.Laliberte for his interest and always helpful assistance.

Acknowledgment is due also to the graduate students Marek Faber and Abdul Hamid for many valuable discussions, encouragment and assistance.

I am forever indebted to my wife Iwona and my son Peter for their patience during this work. I wish to express particular thanks to them.

TABLE OF CONTENTS

LIST OF FIGURES

Page

LIST OF TABLES

CHAPTER 1

INTRODUCTION

The technology for the measurement of the dielectric parameters has been highly developed in recent years. It is customary to make such measurements at discrete frequencies. This requires a trained operator to execute some crucial adjustments, depending on the technique employed at each frequency. The time taken in manipulations, and conversion of the results into usable form, make such technique very laborious. Especially, at the low frequency range of the spectrum such measurements become extremely time consuming due to large period of the exciting wave. The rate of sweeping of the oscillator covering the required frequency range must be slow in comparison with the wave cycle, which also increases the measurement time.

When the results of a variation of dielectric parameters have to be evaluated quickly and often, it becomes necessary to look for a faster method of measurement.

The step-response method, or transient-method, does not suffer from these problems. A single voltage step function is used for excitation of the dielectric material, and its time response is measured. The Fourier transform converts results from the time to frequency domain. It should be emphasised, that the data covering the whole range of frequencies is obtained within duration of a single voltage step, therefore, the measurements at very low frequencies have enormous advantage of speed.

In this project, a system employing the principle of the transient method has been developed. A sampling system has been designed and constructed for measurement of the time--response of a capacitor containing a dielectric material to a single voltage step. Sixteen samples from the response curve are taken at logarithmically spaced time intervals with the base of 2.

The first sample is recorded at 10 μs after applying the voltage step exciting the dielectric. Due to limited conversion speed and accuracy of analog to digital converters, typical sampling circuitry employing a separate voltage step for recording each data had to be built. The last sampling time is equal $/2^{15}$ x 10/ μs.

Using appropriate Fourier transforms, the results of the relative permittivity and loss factor can be calculated at sixteen discrete frequencies spaced at octave intervals. The measurement covers the frequencies from 0.5 Hz to 16 kHz. The time taken to record data by sampling system is approximately 30 sec.

SOME PROPERTIES OF DIELECTRICS

2.1. Basic parameters and background material

The a-c characteristics of materials can be defined in terms of circuit theory concepts /1/. The interaction of electromagnetic field with dielectric material can be described using condenser and coil to separate the influence of electric and magnetic fields.

2.1.1. Permittivity

A capacitor, connected to a sinusoidal voltage source $V = V_o e^{j\omega t}$ of the angular frequency $\omega = 2\pi f$, stores, when vacuum is its dielectric, a charge $Q = C_o V$ and draws a charging current

$$I_c = \frac{dQ}{dt} = j\omega C_o V \qquad /2.1/$$

This current is leading the voltage by a temporal phase angle 90^o /Fig.2.1/. C_o is the vacuum or geometrical capacitance of the condenser.

When filled with some substance, the condenser increases its capacitance to

$$C = C_o \frac{\varepsilon'}{\varepsilon_o} = C_o \varepsilon'_r \qquad /2.2/$$

where ε' and ε_o designate the real permittivities or dielectric constants of the dielectric and of the vacuum, respectively, and their ratio ε'_r the relative dielectric constant of the material / $\varepsilon_o = 1/36\pi \times 10^{-9}$ farad/m/.

Simultaneously, there may appear, in addition to the charging current component I_c, a loss current component

$$I_l = \sigma_c V \qquad /2.3/$$

in phase with the voltage, where σ_c represents the conductivity associated with conduction current in the dielectric.

The total current traversing the condenser

$$I = I_c + I_l = /j\omega C + \sigma_c/ .\ V \qquad /2.4/$$

is inclined by a power factor angle $\Theta < 90^{\circ}$ against the applied voltage V, that is, by a loss angle δ against +j-axis /Fig.2.2/.

The frequency response of this current, which can be expressed by the ratio of loss current to charging current, that is, loss tangent $\tan\delta$ as

$$\tan\delta = \frac{I_c}{I_l} = \frac{1}{RC\omega} \qquad /2.5/$$

may not at all agree with that actually observed because the conductance term need not stem from migration of charge carriers, but can represent any other energy-consuming process. It has become customary to refer to the existence of a loss current in addition to a charging current, by the introduction of the complex permittivity

$$\varepsilon^{*} = \varepsilon' - j\varepsilon'' \qquad /2.6/$$

The total current I, may thus be rewritten as

$$I = /j\omega\varepsilon' + \omega\varepsilon''/ \frac{C_o}{\varepsilon_o} V = j\omega C_o \varepsilon_r^{*} V \qquad /2.7/$$

where

$$\varepsilon_r^{*} = \frac{\varepsilon}{\varepsilon_o} = \varepsilon_r' - j\,\varepsilon_r'' \qquad /2.8/$$

is the complex relative permittivity of the material, and ε'' and ε_r'' are the loss factor and relative loss factor, respectively. The loss tangent becomes

$$\tan\delta = \frac{\varepsilon''}{\varepsilon'} = \frac{\varepsilon_r''}{\varepsilon_r'} \qquad /2.9/$$

Since a parallel - plate condenser of the area A and the plate separation d, has the vacuum capacitance

$$C_o = \frac{A}{d}\,\varepsilon_o \qquad /2.10/$$

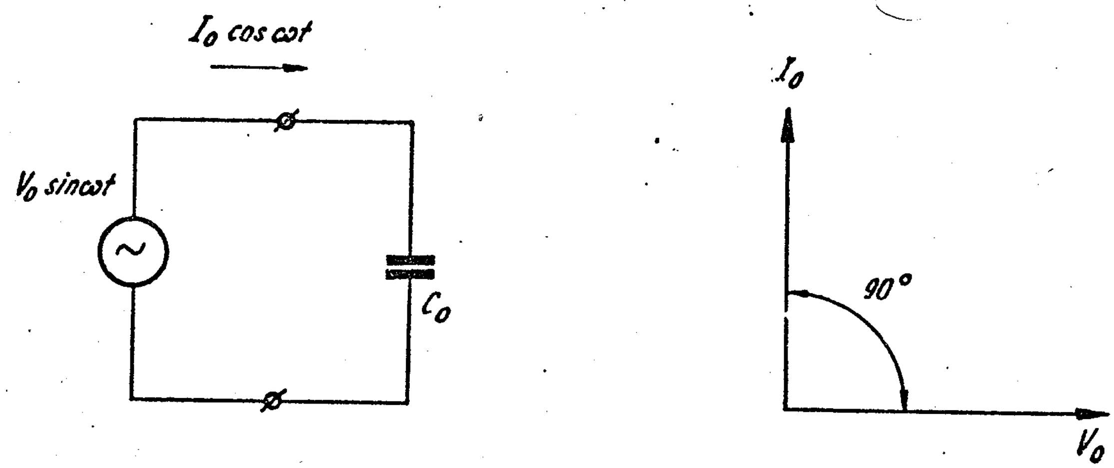

Fig. 2.1 Current-voltage relation in ideal capacitor

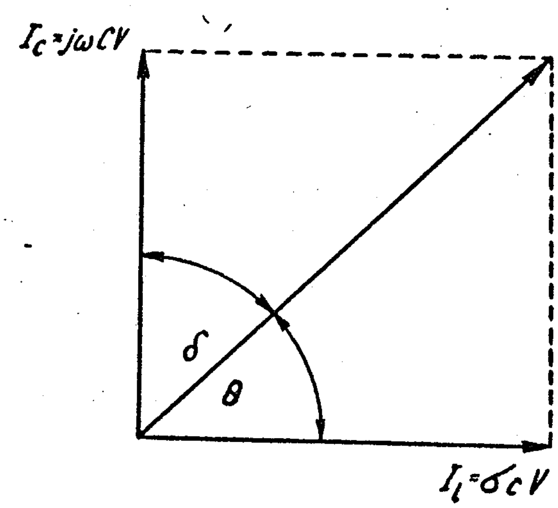

Fig. 2.2 Capacitor containing dielectric with d-c loss

the current density J traversing a condenser under the applied field strenght E = V/d, becomes

$$J = /j\omega\varepsilon' + \omega\varepsilon''/E = \frac{dE}{dt} \qquad /2.11/$$

The product of angular frequency and loss factor is equivalent to a dielectric conductivity

$$\sigma = \omega\varepsilon'' \qquad /2.12/$$

This dielectric conductivity sums over all disspative effects and may represent an actual conductivity caused by migrating charge carriers and an energy loss associated with a frequency dependence (dispersion of ε' for example).

2.1.2. Permeability

If the dielectric material is transferred from the electric field of the capacitor into the magnetic field of a coil, the voltage V drives through the coil a magnetization current I_m according to Faraday's inductance law

$$\bar{I}_m = \frac{V}{j\omega L_o \frac{\mu'}{\mu_o}} \qquad /2.13/$$

where L_o represents the vacuum or geometrical inductance of the coil. This magnetization current lags behind the applied voltage by 90^o. The permeabilities μ', and μ_o designate the magnetization of the material and of the vacuum, respectively, and their ratio μ'/μ_o the relative permeabilty of the material in which the magnetic field of the coil resides / $\mu_o = 4\pi \times 10^{-7}$ H/m/.

Because of the resistance R of the coil windings, an ohmic current component V/R exists. In addition, there may appear, in phase with V, a magnetic loss current I_1 caused by energy disspation during the magnetization cycle.

In complete analogy to the dielectric case a complex permeability is introduced

$$\mu^* = \mu' - j\mu'' \qquad /2.14/$$

The complex relative permeability is

$$\mu_r^* = \frac{\mu}{\mu_o} = \mu_r' - j\mu_r'' \qquad /2.15/$$

Thus the total magnetization current is

$$I = I_m + I_1 = \frac{V}{j\omega L_o \mu_r^*} \qquad /2.16/$$

2.1.3. Frequency behaviour

Values for dielectric properties of most materials are very much dependent upon the frequency of the alternating field. According to previous considerations, the macroscopic behaviour of a dielectric material is determined by the two complex parameters ε^* and μ^*.

For most materials other than ferromagnetic substances, μ^* has essentially the value of μ_o, and this holds true for biological materials and agricultural products.

Discussions of the anomalus dispersion /the decreasing of ε', with increasing frequency/ and the dielectric theories of Debye, Osanger, Cole, Kirkwood, Fröhlich, and others, are found in many references /1/, /2/, /12/. Basically, all of these formulations recognize a contribution to the dielectric constant of materials containing molecules with electric dipole moments, through the polarization, resulting from the orientation of the dipoles with the applied electric field. Two lesser contributions to the polarizability arise from electronic polarization, and atomic polarization. These two types of polarization are termed "deformation" polarization.

As frequency increases from low values, the polar molecules can follow the changes in direction of the electric field up to a point, and, as frequency continues to increase, the dipole motion can no longer keep up with the changing field. As a result, the dielectric constant drops with increasing frequency in this region, and energy is absorbed, as a result of the phase lag between the dipole rotation and the field. The relationship between the dielectric constant and loss factor is illustrated in Fig.2.3. Debye /1929/ developod the mathematical formulation which can be expressed as

$$\varepsilon_r^* = \varepsilon'_{r\infty} + /\varepsilon'_{rs} - \varepsilon'_{r\infty}//\!/1 + j\omega\tau/ \qquad /2.17/$$

where ε'_{rs} is the static or d-c value of the dielectric constant, $\varepsilon'_{r\infty}$ is the infinite frequency or optical value, and τ is the relaxation time. The loss factor, ε''_r, peaks at the relaxation frequency $\omega = 2\pi f = 1/\tau$. At this frequency, ε''_r has the value $/\varepsilon'_{rs} - \varepsilon'_{r\infty}//2$ and ε'_r has the value $/\varepsilon'_{rs} + \varepsilon'_{r\infty}//2$.

The dispersion of some pure liquids closely follows Debye equations.

It was noted by Cole and Cole, that plotting ε'_r and ε''_r in the complex plane in accordance with the Debye relation, results in a semicircle /Fig.2.4/.

The modified equation presented by Cole and Cole /1941/, results in a Cole - Cole plot, which is an arc of a circle with the center below the $\varepsilon''_r = 0$ axis /Fig.2.5/.

$$\varepsilon_r^* = \varepsilon'_{r\infty} + \frac{\varepsilon'_{rs} - \varepsilon'_{r\infty}}{1 + /j\omega\tau/^{1-\alpha}} \qquad /2.18/$$

α is the empirical relaxation - time distribution parameter and takes values between 0 and 1.

Several other models have been developed to explain the behaviour of certain types of materials. One known as the Cole - Davidson representation, results in a skewed arc

/Fig.2.6/, and mathematically it is defined as

$$\varepsilon_r^* = \varepsilon'_{r\infty} + \frac{\varepsilon'_{rs} - \varepsilon'_{r\infty}}{/1 + j\omega\tau/^{\beta}} \qquad /2.19/$$

where β is restricted to values between 0 and 1.

The incidence of d-c conductivity appears as a distorting feature plotting ε'_r and ε''_r in the complex plane. This is shown in Fig.2.7. The constancy of $/\varepsilon'' \times f/$ at low frequencies provides one of the best methods of evaluating conductance in poorly conducting media.

2.2 Biological materials as dielectrics

Generally, for biological materials and agriculture products $\mu^* = \mu_0$ and therefore the dielectric constant versus frequency dependence becomes of first interest in dielectric studies.

Another absorption process is likely to be present in agricultural products /10/, especially, at low frequencies /below 1kHz /2//. The general aspects of this absorption were evaluated by Wagner, and the dielectric effect is referred to, as Maxwell - Wagner absorption. It results from polarizations at interfacial boundaries and occurs in nonhomogeneous materials. The frequency character of the process is identical with that of the simplest /Debye/ dipolar absorption, and many biological specimens show it. The process is far more common in solid materials. In addition, energy dissipation can occur due to d-c conductivity of the medium and electrode polarization effects. Especially, this appears in systems which have an ionic conductance. Not infrequently, all these processes and dipolar absorption will occur simultaneusly, making dielectric studies particulary troublesome in this frequency range.

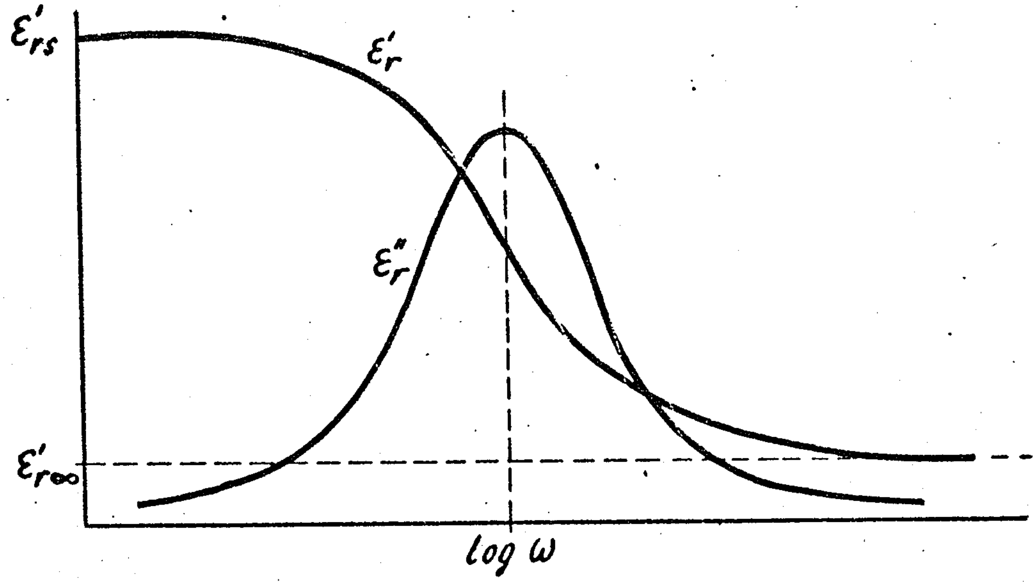

Fig. 2.3 Dispersion and absorption curves for a polar material following the Debye relaxation process

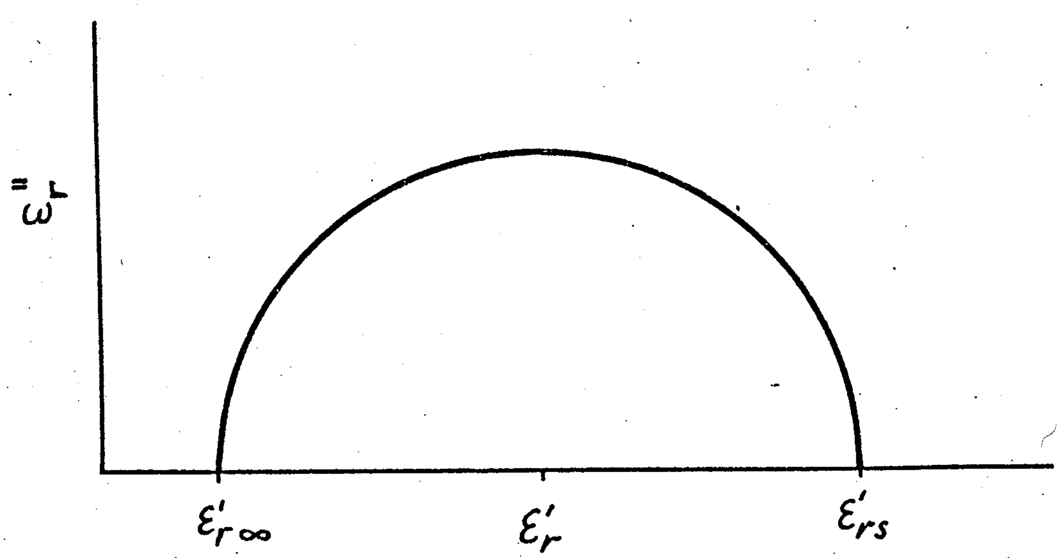

Fig. 2.4 Cole-Cole plot for Debye relation

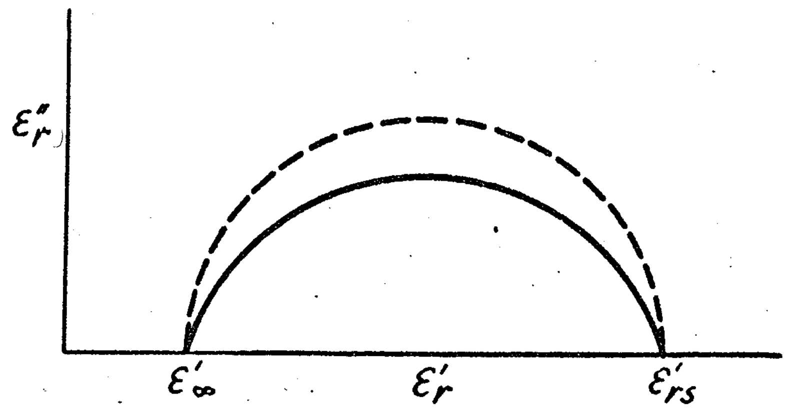

Fig. 2.5 Cole-Cole circular arcs

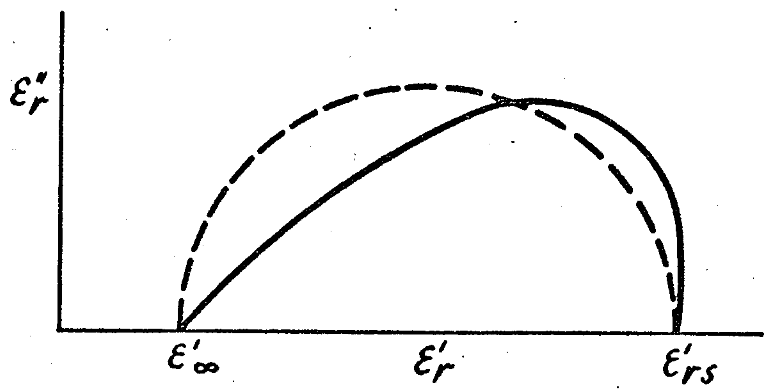

Fig. 2.6 Cole-Davidson skewed arcs

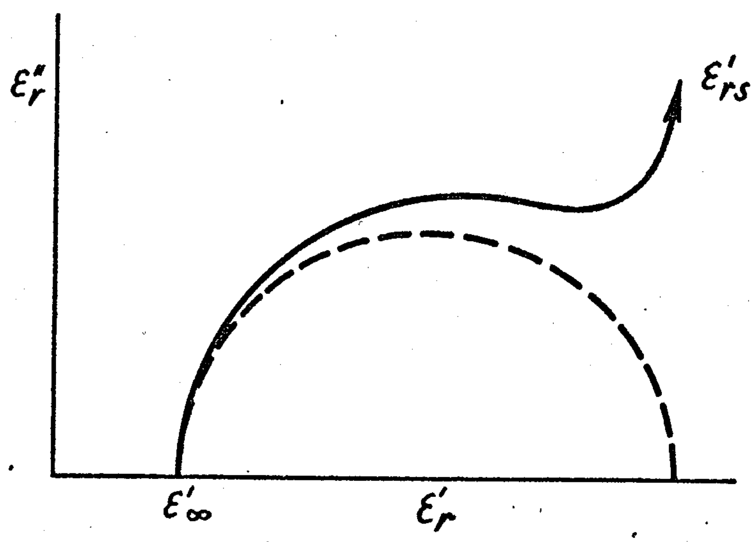

Fig. 2.7 Cole-Cole plot for dielectric with d-c conductivity

CHAPTER 3

EXPERIMENTAL TECHNIQUES

For many applications some knowledge is essential concerning dielectric properties of materials being considered. Since the dielectric properties vary with frequency, their frequency dependence may be necessary for a particular application.

Dielectric measurement may be made over a very wide range of frequency, from the microwave region, through the radio- and audio- frequency regions, down to very low frequencies.

Many methods have been developed for determining dielectric properties of materials depending on the frequency range. For the microwave region /up to 18×10^9Hz/, a time-domain technique performed by means of fast rise time pulse, and high frequency sampling oscilloscop, is very useful/11/. Resonant circuit are used successfully at the radiofrequencies /10^5 - 10^8Hz/. Lower frequencies can be investigated using two basic approaches to the problem,the steady-state technique, and the transient technique.

3.1 Steady-state method

This method is very widely used at present time.Generally, it employs a specially constructed sample holder capacitor, which is used with an impedance bridge and generator, to measure changes in capacitance and dissipation factor due to presence of the sample material. From these electrical measurements and the volume of the sample in the sample holder, the dielectric properties are calculated.Fig. 3.1 shows basic diagram of the measuring circuit. It is usual for such measurements to be made at discrete frequencies only, and a trained operator is almost always needed to execute some crucial adjustment procedure at each frequency.

Until fairly recently, the lowest frequency, obtainable with conventional bridges had been about 10 Hz using Schering bridge /2/. Special bridges supplied with a motor driven potentiometer have been used down to about 0.1 Hz /6/. The frequencies of interest are often so low, that steady-state measurement becomes extremely time consuming, as the rate of sweeping oscillator must be slow, in comparison with the period of the exciting wave. The scarcity of skilled operators, and the time taken in manipulations, make this method increasingly incompatible with the needs, when the results of a variation of the dielectric properties may have to be evaluated quickly and often.

3.2 Transient method

The transient method or step response method does not suffer from these problems. The principle of operation, is to record a time response to a voltage step of a capacitor containing a sample of measured material /Fig.3.2/.
It should be ephasised, that the excitation is by a simple voltage step function, and the response measured within duration of the single step is used as a data, to cover the whole range of frequencies.

For a capacitor having unity vacuum capacitance, filled with the material as dielectric, the current response i/t/ to a unit voltage step, is connected with complex permittivity by the Fourier transform /3/.

$$\varepsilon^*/\omega/ = \varepsilon'/\omega/ - j\,\varepsilon''/\omega/ = \int_0^\infty i/t/\exp/-j\omega t/dt \qquad /3.1/$$

A major practical difficulty in using this method to obtain steady-state information is recording of the i/t/ at both small and large values of time due to some technical reasons.

It means, that any experimental data will cover only a finite range of time, and errors will therefore arise owing to cutting off of the Fourier transform integral at both sides. The magnitude of such errors will depend on the time range of available data, and the value of ω in relation to the minimum and maximum values of time. Hence, it may be inferred, that the wider range of time that the data cover, the wider range of ω is described by, and the $\varepsilon(\omega)^*$ is known more accurately. Ignoring other benefits, this alone emphasises the importance of obtaining time response data over as wide a range of time as possible.

A disadvantage of the transient method is that it can not be applied easily to materials which show significant nonlinearity; fortunately, using even moderately high amplitude of step voltage, most of them are not intended do so.

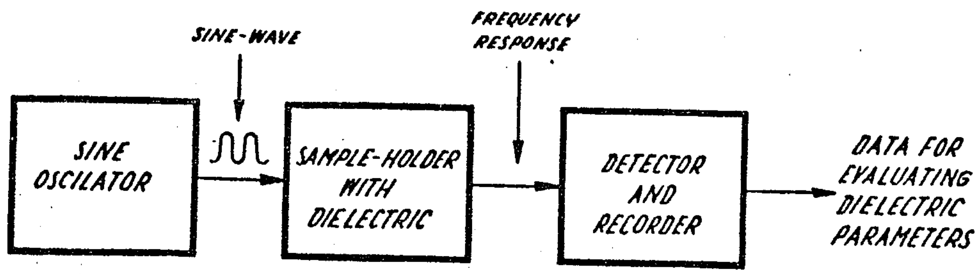

3.1 Basic diagram of the measuring circuit for steady-state technique

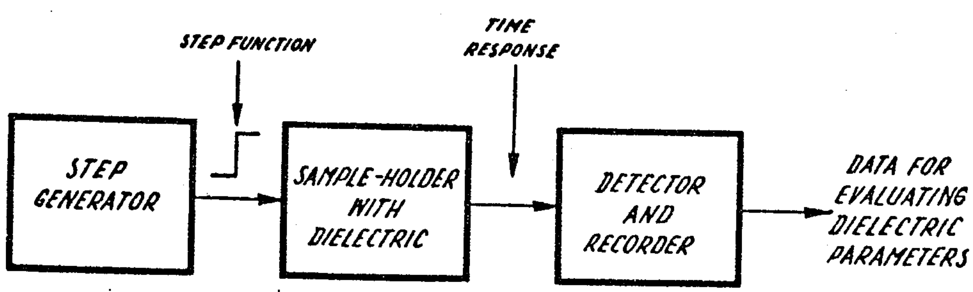

3.2 Basic diagram of the measuring circuit for transient technique

CHAPTER 4

DEVELOPMENT OF EXPERIMENTAL EQUIPMENT

4.1 General design approach

The design and development of the measuring system requires consideration of many different aspects.

The experimental system should provide fast measurement of dielectric properties of many materials. Further, the system should be characterized by simplicity of operation and computer compatible output for easy data processing. Comercially available equipment should be utilized wherever possible.

The construction of a sample-holder for dielectric specimens should facilitate its filling with granular materials.

The design of the system has been based on principles of transient method, as the frequency range of interest is from kHz region down to very low frequencies.

4.2 Measuring system

A simplified block diagram of the system which has been developed is shown in Fig.4.1.

A step voltage produced by HP 8003A pulse generator is, applied to the sample of a dielectric specimen placed in the sample-holder capacitor. The output pulse exciting the dielectric is triggered from the control circuit.
This pulse has 5ns rise time and its duration can be adjusted up to 3 sec. Maximum output amplitude is $\pm$ 5 V across a 50 ohms load impedance.

A HP 3480A digital voltmeter combined with HP 5055A digital recorder have been used as the recording equipment. These instruments provide a high performance economical method of making permanent records of digital data.
The voltmeter has 950 μs reading time and $\pm$ /0.01% of reading + 0.01% of range/ voltage accuracy. An external trigger

from control circuit assures reading, when the sample-hold system is in the hold mode. Output information from the voltmeter is available in the BCD and together with print command is interfaced with the recorder. Permanent records of data are printed on paper tape.

The part of the system which has been designed and built consists of:

- Sample-holder Capacitor
- Input Amplifier and Sample-hold Circuit
- Control Circuit

These units have been developed to cope with the requirements for the experimental system, and more detailed discussion is devoted to them.

It should be pointed out that the use of the system is very simple. All the control signals are performed automatically in order to obtain fast measurement and simplicity of operation.

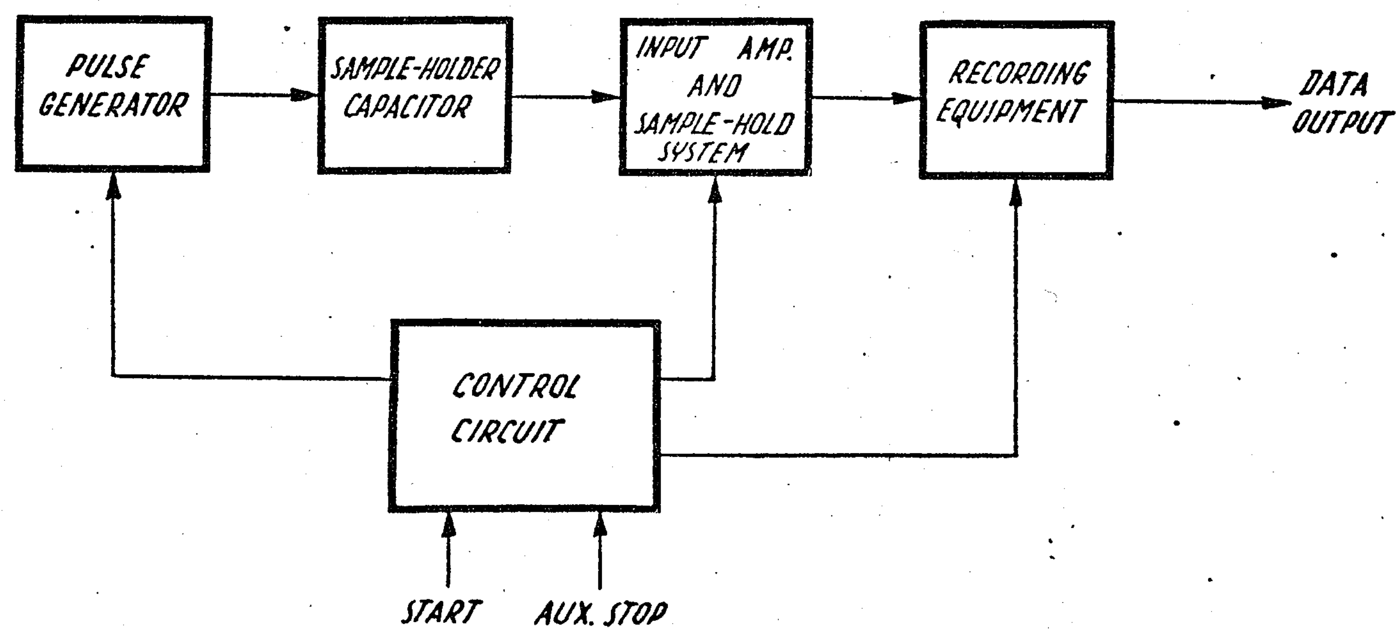

Fig. 4.1 Block diagram of the measuring system

4.2.1 Sample-holder Capacitor

A coaxial design was selected for the sample-holder capacitor. Fig.4.2 shows a sectional view of the constructed capacitor with its important dimensions. This type is easy to fill quickly and uniformly with granular material, as grain for instance. Copper tubing with 1/8-in. walls available in 2 and 3-in. outside diameters was used for the electrodes. The tube which formed the inner electrode was closed at the bottom by a copper plate and capped on the top by a right circular conical surface. Spacing between the electrodes was maintained by a base plate machined from teflon to hold the electrodes in coaxial relationship.

A mounting block from teflon was constructed to support the sample-holder capacitor and facilitate electrical connection to the input of the measuring circuit. Brass jacks with banana plugs were used to provide easy removing of the capacitor.

The value of the air capacitance of the sample-holder is 44 pF and fits theoretical results.

It was found /3/, /5/, /6/, that the larger value of the sample-holder capacitance provides better sensitivity measurement at lower frequencies. Because a certain distance is required between electrodes for granular type of a dielectric specimen, increase of the air capacitance causes rapid increase of the capacitor size.

Consequently, depending on the dielectric material 10^{-1} Hz has been estimated as the lowest frequency since the resolution of the system limits the recording of valuable data.

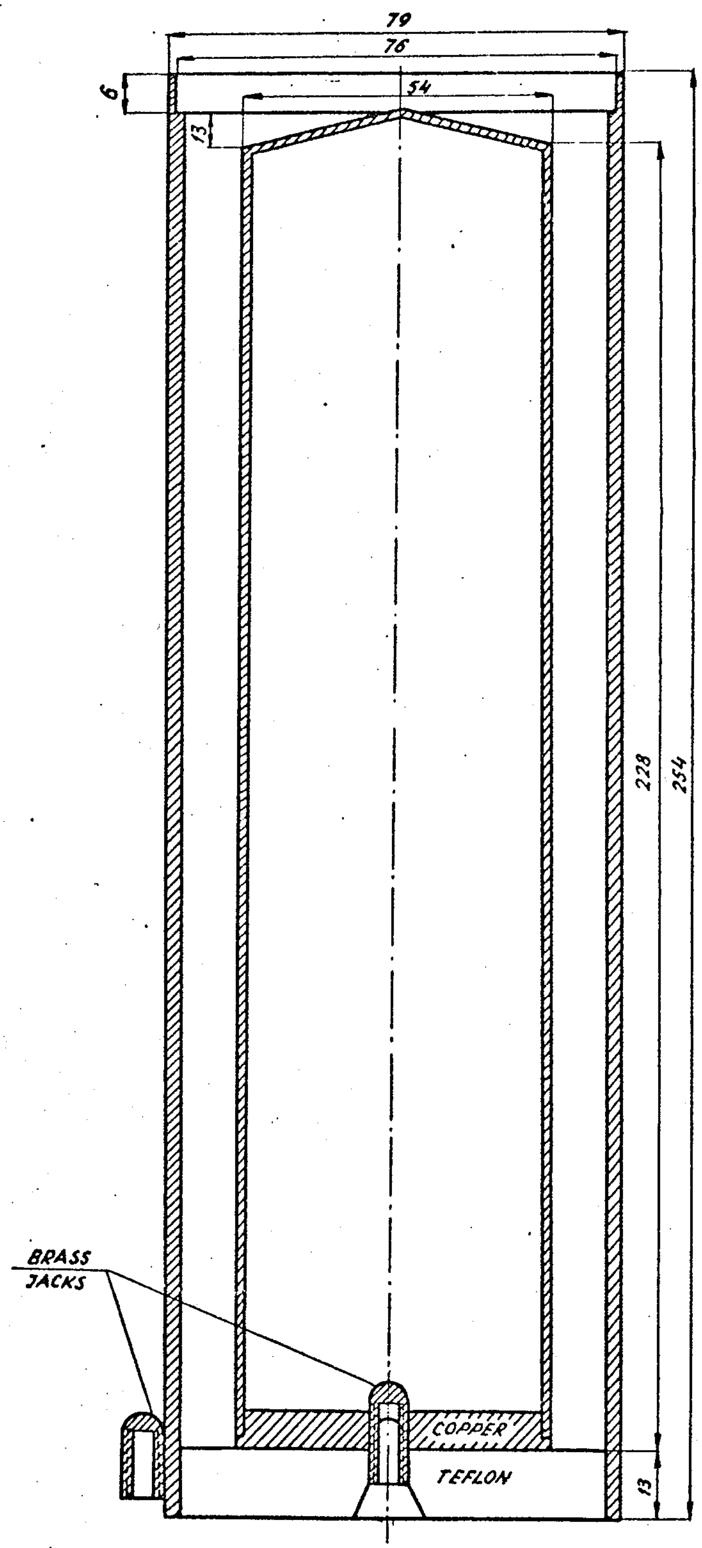

Fig. 4.2 Sample-holder Capacitor

4.2.2 Input Amplifier and Sample-hold System.

The basic diagram of this unit is shown in Fig.4.3; a detailed schematic is presented in Appendix.

The input of the circuit is connected directly to the sample-holder capacitor, therefore influence of the input impedance must be taken into consideration.

A Burr-Brown 3307/12C operational amplifier was used as the input amplifier. This is effectively an electrometer with the full power sine wave bandwidth of 100 kHz and very high FET-input impedance of 10^{11} ohms. The unity gain buffer input amplifier is used to buffer the sample-holder capacitor in a long-term sample/hold operation. Combined with Burr-Brown SHM 41 sample and hold module, this unit provides a simple system for data digitaiting.

The reed switch connected in parallel to the input, and, when closed, discharges the sample-holder and prevents storing of the charge in the specimen while it is being stimulated by succesive pulses during each sampling period. When opened, it introduces 10^{14} ohms resistance and does not cause decay of the voltage on the sample-holder capacitor.

Control signals to operate the sample and hold system and reed switch are provided from the control circuit.

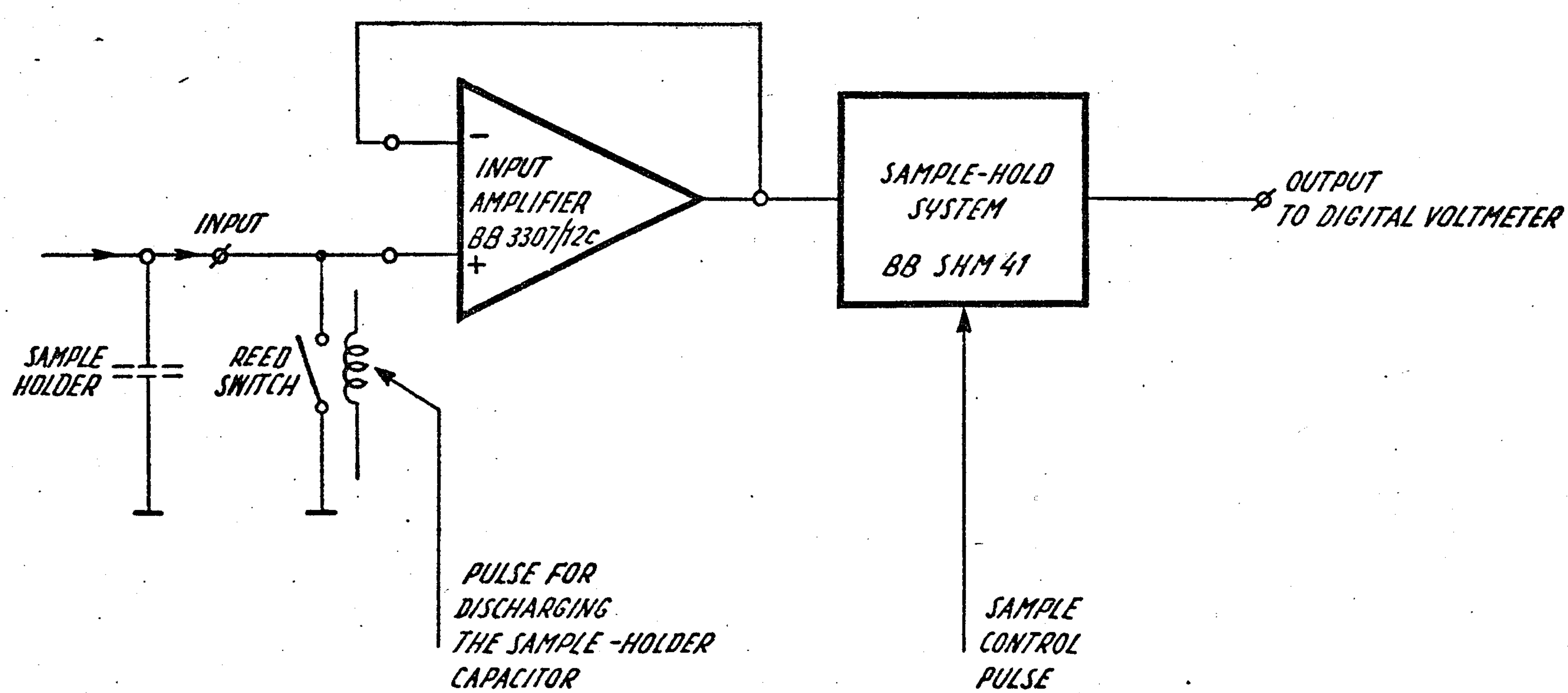

Fig. 4.3 Input Amplifier and Sample-hold System

4.2.3. Control Circuit

This part of the experimental system is most complex; therefore, many problems required special attention during the design procedure.

The control circuit executes control signals for the entire measuring system. More specifically the objectives are:

1. To trigger the pulse generator and initiate the measurement,
2. To generate a sampling pulse for the sample and hold system,
3. To trigger the digital voltmeter when the response is sampled and held, and
4. To turn on the reed switch and discharge the sample-holder capacitor, after the data has been recorded.

The commands performed by the control circuit during each sampling period are shown in Fig. 4.4.

The principle of typical sampling method has been employed due to overall performance of analog to digital converters /15/. Their accuracy and speed of operation limits the frequency range for a particular application.

A basic idea is to take one sample from the response from each of a succession of step voltages spaced by a certain period of time. When the sample is held, accurate analog to digital conversion can be easily performed, since short conversion time is not longer important.

The measurement time consists of sixteen successive sampling periods spaced by about 2 sec. Only one data is recorded during each sampling period at time $t = t_o \times 2^n$, where t denotes sampling time, t_o the first sampling time, and n the sampling period number. For simplicity of operation, all the control functions are executed automatically by the control circuit, and complete measurement time takes approximately 30 sec.

The problem of selecting the sampling times requires a special consideration. It is apparent that the number of samples and their sampling times should be selected for each specific application.

An attempt is given here to justify the choice of those important parameters.

In the dielectric case, a voltage step applied to the specimen results in a monotonically decaying current. This current response is related to the complex permittivity of dielectric by the Fourier transform /Eg. 3.1./.

If, for example, the frequency range of interest covers six decades, the measurement in the time domain should be made over at least six decades of time to obtain data for the Fourier transform. However, for the achievable ratio of 10^6 between the upper and lower values of time, it would be necessary to store a million values of data using evenly spread samples. Thus it is obvious that a more economical way of storing such a quantity of data must be sought.

It is commonly observed in practice that the time integral of monotonically decaying current charging the specimen also behaves monotonically and is very approximately linear with respect to the logarithm of time /3/, /4/. Hence, if a sufficiently small logarithmic base is chosen, values of a total charge observed at equal intervals of log /t/ can provide the required economical record of a wide-range of step-response data. A base of 2 is chosen here, as it is easily compatible with digital circuits.

The value of first sampling time t_o is limited by the bandwidth of input amplifier and the acquistion time of sample and hold system. For a 100 kHz bandwidth and a few µs acquisition time, t_o = 10 µs has been chosen. Selection of t_o sets the time scale of the measurement.

To reduce error due to limited acquisition time of B-B SHM 41, especially at the small times of the response, a modification of the sampling pulse has been introduced. Now, the input of sample and hold system tracks the measured signal until the sampling time t in each of the sampling periods to increase the aperture time.

The last sampling time is $t = t_o \times 2^{15} = 327.68$ ms, and denotes the time range over which the response is recorded. Longer times are found to be not feasible to measure due to resolution of the system for a given size of sample-holder capacitor and input circuitry performance.

The block diagram of the control circuit is shown in Fig.4.5 while a schematic is presented in Appendix. Generally, the TTL integrated circuits have been used. The operation of the circuit is as follows:

A standard frequency f of 10 MHz is produced by Crystal Oscillator used as a clock. Its short-term frequency stability is better than 10^{-7} per minute. This signal is then converted to a square wave by Schimdt Trigger 7413 and divided by two Decade Counters 7490 to obtain the value of $t_o = 10$ µs. Next, the signal goes through a 16-bit binary counter so sixteen standard frequencies decreasing by a factor of 2, are available in its output. These signals are selected by Data Selector 74 150 and used then as a sampling pulses.
The Data Selector converts parallel binary information to a serial form by means of a select signal supplied from the Control Data 7493. Clearly, the Data Selector enables choosing only one of the sixteen standard frequencies which occur on its data inputs simultaneously. After the sampling pulse has been generated, the Control Data counter inhibits all the data inputs exceptfor the next one, so the two times larger time can be chosen and the next sampling pulse

can be produced. The Monostable Multivibrators 74 121 were used as an output devices to obtain all required triggering pulses for the entire measuring system. The D-type Flip-Flops 7474 facilitate "Start", manual or automatic "Stop", as well assure synchronization between standard frequency and gate control signal. The main gate consists of Nand Gates 7400.

The finite value of clock frequency stability /10^{-7}/ and the propagation time for the employed TTL technique /typical, 10 ns per gate/, introduces a certain delay and jitter of the sampling time t. These, give an occasion to rise an error in data digitaising, which is most effective at $t_o = 10$ µs.

It is easy to notice that the error due to the above reasons, can be neglected at first approach. More detailed, the delay caused by the propagation time of the TTL circuits can be easily compensated by proper lenght of the external 50 ohms coaxial cable, by means of which the step pulses are applied to the specimen.

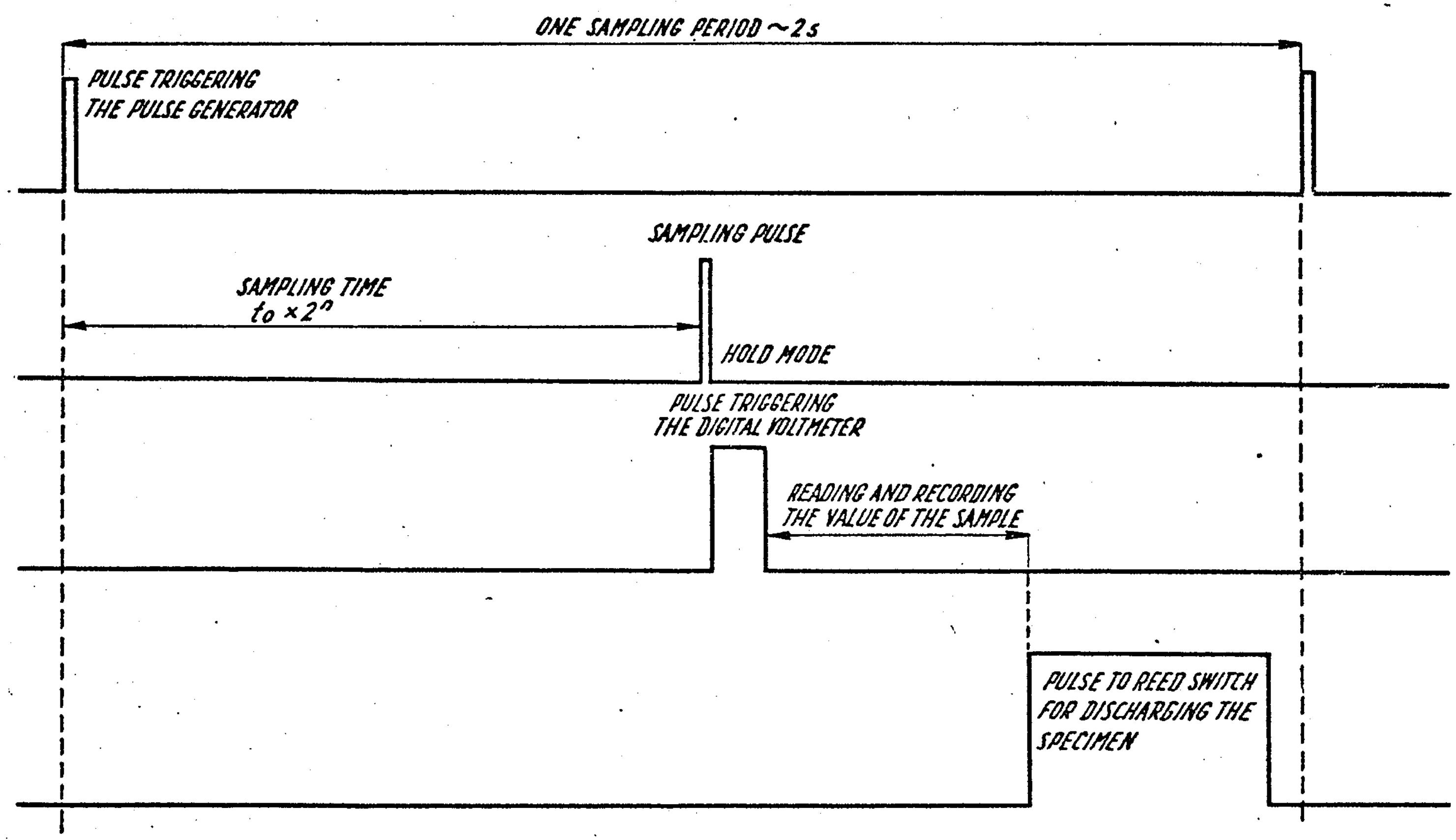

Fig. 4.4 Commands performed by control circuit during each sampling period

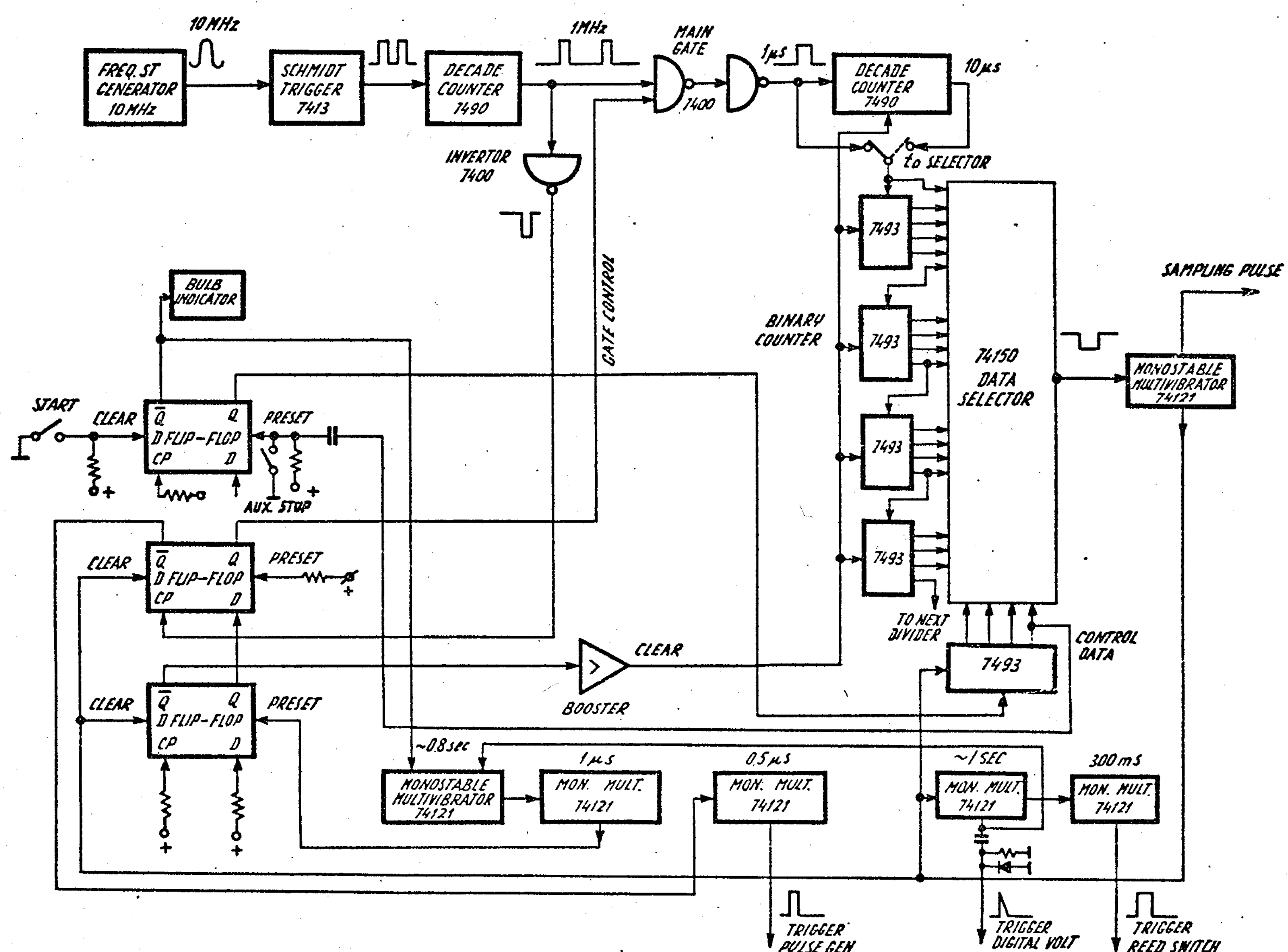

Fig. 4.5 Block Diagram of the Control Circuit

CHAPTER 5

TRANSFORMATION TO THE FREQUENCY DOMAIN

5.1 Fourier transformation of logarithmically spaced data

Values of current i/t/ recorded at equal intervals of log /t/ provide the required data for computation of $\varepsilon(\omega)^*$. The simplest way of transforming to the frequency domain is to first recover the i/t/ data in linear time from the logarithmic representation, and then to apply the Fourier transform to them.

Recalling that the time integral q/t/ of the current i/t/, is very linear with respect to the logarithm of time /3/, it is convenient to perform direct transformation from the logarithm time domain to the logarithm frequency domain. This gives additional advantage since the relaxation regions for dielectrics are usually described with respect to the logarithm of frequency.

Fig. 5.1 shows the function q/log /t// around any particular sampling time t_1. The assumption of linearity of q with log/t/ over the octave time interval gives the equation

$$q = q/\frac{t_1}{\sqrt{2}}/ + \left\{ q/\sqrt{2}t_1/ - q/\frac{t_1}{\sqrt{2}}/ \right\} \log_2 /\frac{\sqrt{2}t}{t_1}/ \qquad /5.1/$$

where q/t/ is a time integral of current through the specimen i.e.

$$q/t/ = \int_0^t i/t/dt \qquad /5.2/$$

and thus the corresponding current is

$$i/t/ = \frac{dq/t/}{dt} = \frac{q/\sqrt{2}t_1/ - q/\frac{t_1}{\sqrt{2}}/}{t \ln 2} \qquad /5.3/$$

The principle may be extended to the rest of the function by splitting it into octave intervals for all t and, in the general interval $nt_1/\sqrt{2}$ to $\sqrt{2}\cdot nt_1$.

Hence $i/t/ = \frac{\Delta q/n/}{t \ln 2}$ /5.4/

for $\frac{nt_1}{\sqrt{2}} \leqslant t \leqslant \sqrt{2} \cdot nt_1$

From eqn. 3.1

$$\mathcal{E}^*/\omega/ = \frac{1}{\ln 2} \sum_{p=-\infty}^{+\infty} \Delta q/n/ \int_{nt_1/\sqrt{2}}^{nt_1\sqrt{2}} \frac{1}{t} \exp /-j\omega t/ dt \qquad /5.5/$$

where $n = 2^p$ and p is an integer between $-\infty$ and $+\infty$.
Eqn. 5.5 may be rewritten in form

$$\mathcal{E}^*/\omega/ \doteq \sum_{p=-\infty}^{+\infty} \Delta q/n/ \left[x/n/ - jy/n/ \right] \qquad /5.6/$$

where $x/n/ = \frac{1}{\ln 2} \int_{nt_1/\sqrt{2}}^{nt_1\sqrt{2}} \frac{\cos \omega t}{t} dt$

$y/n/ = \frac{1}{\ln 2} \int_{nt_1/\sqrt{2}}^{nt_1\sqrt{2}} \frac{\sin \omega t}{t} dt$

thus the transforms have the forms

$$\mathcal{E}'/\omega/ = \sum_{p=-\infty}^{+\infty} \Delta q/n/ \cdot x/n/ \qquad /5.7/$$

$$\mathcal{E}''/\omega/ = \sum_{p=-\infty}^{+\infty} \Delta q/n/ \cdot y/n/ \qquad /5.8/$$

The constant coefficients x/n/ and y/n/ calculated for various values of $n\omega t_1$, where $\omega t_1 = 1$, are listed in Table 5.1. The computer program representing these transforms is enclosed in appendices.

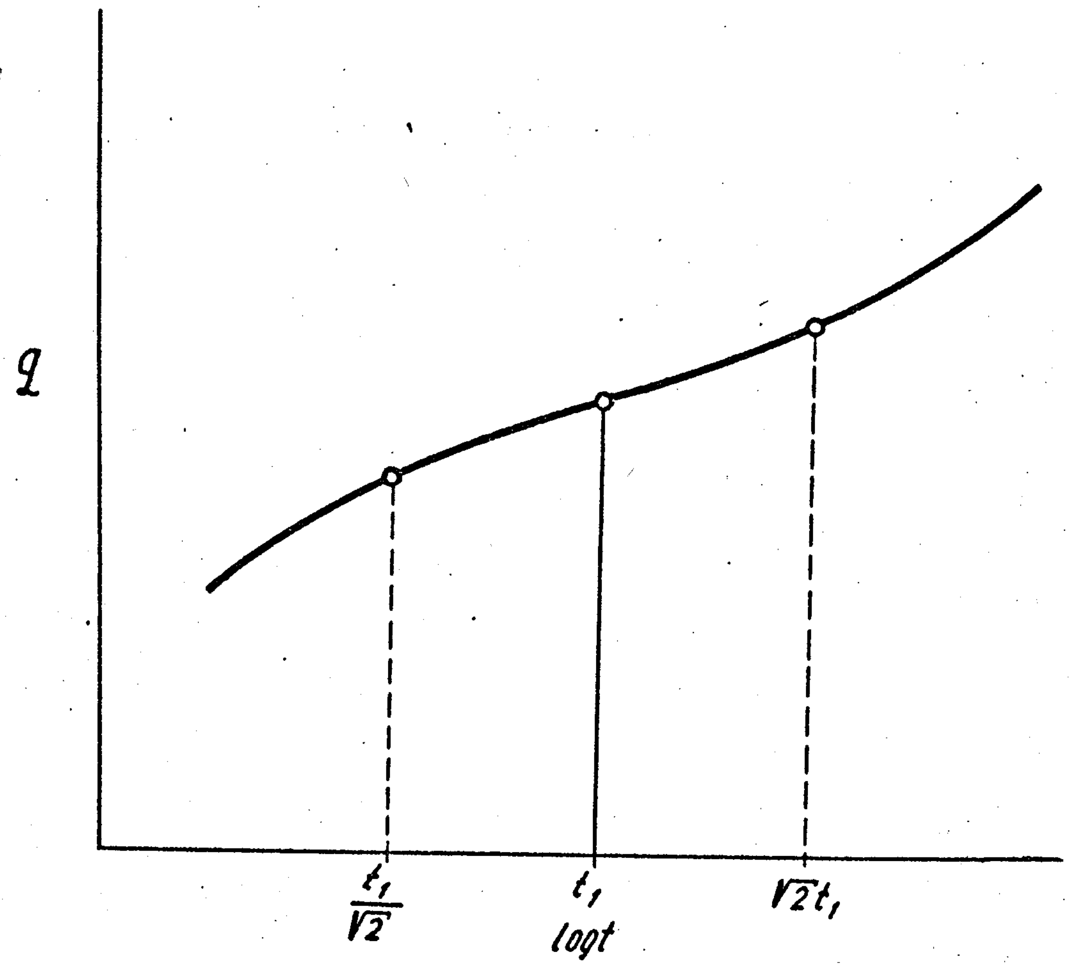

Fig. 5.1 Function to be approximated to around the sampling time t_1

Table 5.1 The coefficients x/n/ and y/n/ used in computer program

p	n	x/n/	y/n/
- 5	1/32	0.9996	0.0319
- 4	1/16	0.9980	0.0638
- 3	1/8	0.9916	0.1271
- 2	1/4	0.9665	0.2519
- 1	1/2	0.8683	0.4858
0	1	0.5128	0.8345
1	2	- 0.4136	0.8212
2	4	- 0.4294	- 0.5552
3	6	0.0514	0.1444
4	8	0.0873	0.0818
5	32	0.0658	- 0.0628

5.2 Accuracy of the measuring system and transforms.

The accuracy of the final values of $\varepsilon^{*}/\omega/$ depends on the precision of measurement of the i/t and on the degree of approximation involved in the use of the transforms from time to frequency domain. Errors in measurement of i/t/ will arise from two major sources: the accuracy of i/t/ in analogue form and the digitising procedure. The significant sources of errors in analogue form can be due to a stray current at the input of input amplifier and due to lack of flatness of the voltage step. Very high input impedance FET aplifier /10^{11} ohms/ was used to reduce the stray current. The error caused by this is less than 1% for the last sampling time /$t=10\times2^{15}\mu s$/. Again, the larger time values of i/t/ are most affected by shape of the step voltage.
It is common, that the output amplitudes of the pulse generators droop almost linearly by a small amount. The error superimposed by the step pulse can be up to 5% with the HP 8003A generator.

When i/t/ is converted into digital form, it is represented by a finite integral number in digital voltmeter. Values of recorded samples can differ from original values. The accuracy now depends on both the sample-hold system and the control circuit. Errors due to accuracy of the digital voltmeter can be neglected, as the small analog to digital conversion time is not longer important.

Largest errors due to the digitising procedure can arise at the beginning of the i/t/, in reverse with the errors due to accuracy in analog form. This is caused by a certain delay and a jitter of the sampling pulse introduced by finite propagation time of the control circuit and standard frequency stability. These errors are not significant and have been evaluated in Chapter 4.

The sample-hold module is a 12-bit system compatible. The error due to this technique is constant, but very small /1/4096/.

The accuracy of appropriate Fourier transforms from time to frequency domain can be evaluated using the most stright forward method. Having the errors incurred in complete record of i/t/, it is very useful in practice to transform the data to the frequency domain and compare the results with the theoretical one for a known material. The analytical evaluation is not an easy task, as the influence of errors involved in measurements in time is spread out over all frequencies.

CHAPTER 6

EXPERIMENTAL VERIFICATION

The performance of the sampling system was verified experimentally by measurement of some electrical parameters of the system, and then the dielectric properties of two different materials.

The basic block diagram of the experimental system is shown in Fig. 6.1. "R" denotes a standard resistor, while "C" either standard or sample-holder capacitor.

Fig. 6.2 shows block diagram of the system used for measurement of the Input-Output characteristic, /Fig.6.5/. The dynamic range of the sampling system was found larger than $\pm$ 10 V and the nonlinearity less than 0.1%.

The system shown in Fig. 6.4 was used to check the sampling times. Although an error equal 2×10^{-5} was found, a detailed discussion should be avoided due to comparable frequency stabilities of the oscillators used in the sampling system and the time counter /10^{-7}/.

The flatness of the voltage step produced by the generator was tested in system shown in Fig.6.3. The maximum droop measured over the complete sampling time range was found less than 1% for the amplitude V_s = 10 V.

The dynamic behaviour of the experimental system was verified by measurement of the voltage responses for some standard values of the time constants.

Table 6.1 shows the computed theoretical values and the experimental results. The overall accuracy was found to be better than 3%. It should be pointed out, that any error introduced by the experimental system is involved in the finite result in this case.

Next, the dielectric properties of two materials were tested and comprised Carbon tetrachloride CCl_4, and a sample of wheat. The measurement procedure was as follows:

The standard resistance R was connected in series with the sample-holder capacitor C, Fig.6.1, to reduce the current charging dielectric specimen.

The experimental results for Carbon tetrachloride are shown in Fig.6.6. The real permittivity of 2.2 was evaluated directly from the time constant since the CCl_4 is a lossless dielectric.

For measurement of the wheat, which is a lossy dielectric, the value of R must be negligible compared to the instantenous impedance of the specimen. The voltage responses for empty and wheat filled sample-holder capacitor were recorded. Different values of R were chosen to fit the dynamic range of the sampling system. The current charging specimen, i /t/, was calculated from the voltage drop across the resistance R. The normalization procedure of the current was necessary for the computer program. Now, the current becomes

$$C\ /N/ \ = \ i\ /t/ \times S \qquad /6.1./$$

where S is a scaling factor. Taking account of the fact that the geometric capacitance of the sample-holder capacitor and the applied voltage step are not unity, the scaling factor is

$$S = \frac{1}{C_a \times V_s} = \frac{10^{10}}{4.4} \qquad /6.2/$$

since $C_a = 44$ pF and $V_s = 10$ V.

The normalized current response for the sample of wheat is calculated in Table 6.2 and shown in Fig. 6.7.

Table 6.3 contains the computer printout of the results in the frequency domain. The results of real permittivity and loss factor for the sample of wheat are plotted in Fig.6.8 and Fig.6.9.

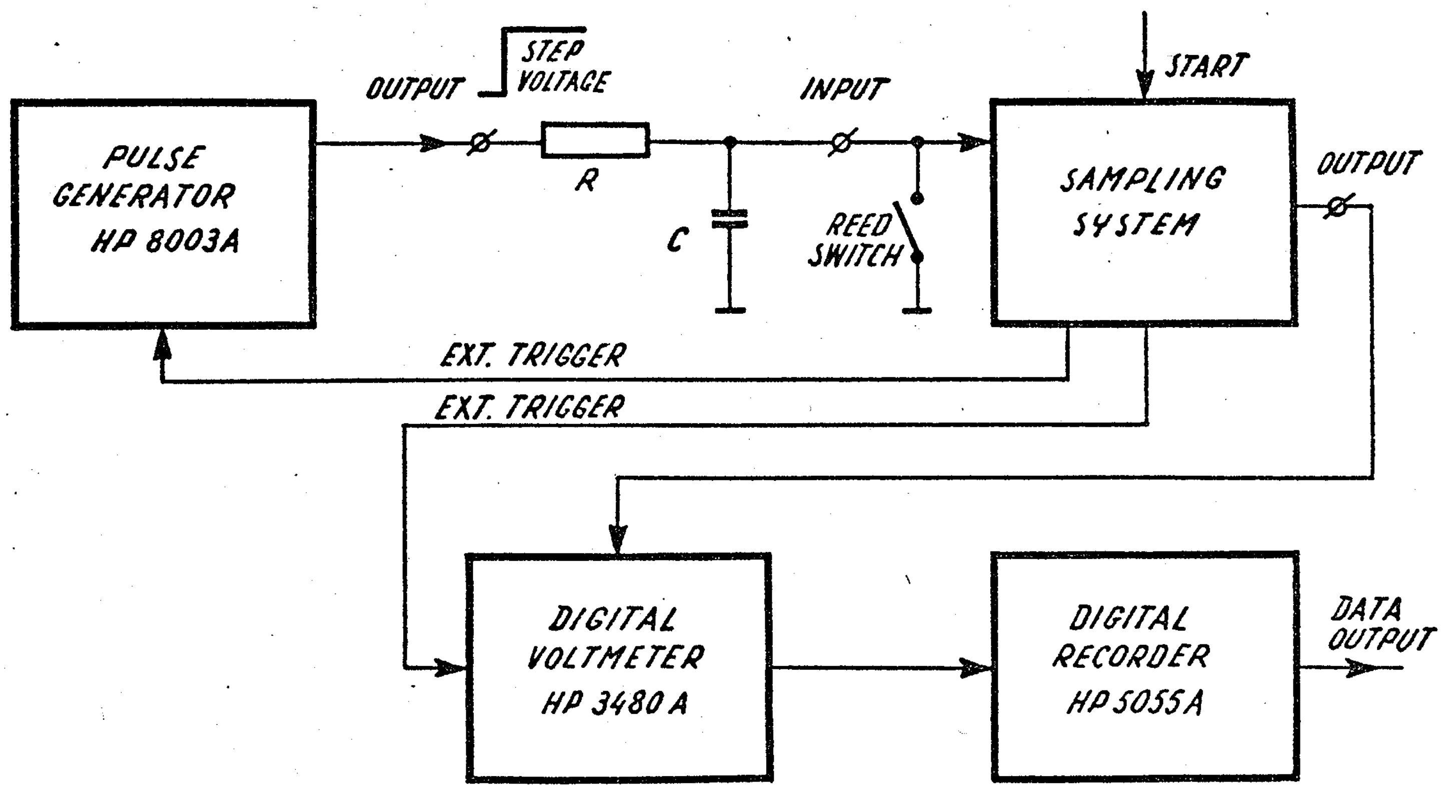

Fig. 6.1 Block diagram of the experimental system

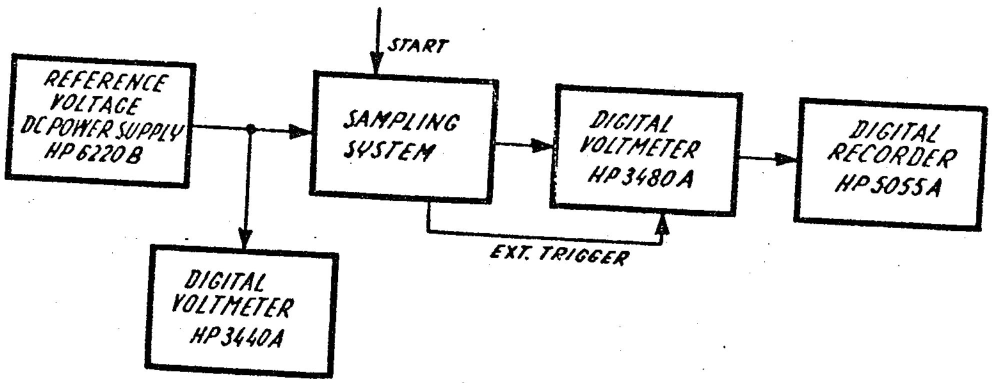

Fig. 6.2 Simplified block diagram for transient characteristic measurement

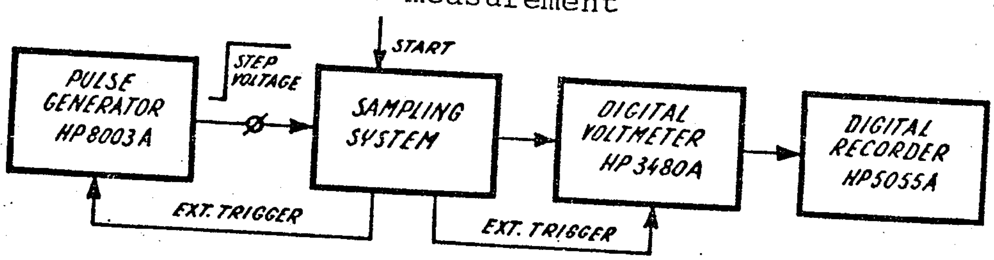

Fig. 6.3 Simplified block diagram for measurement of the voltage step flatness

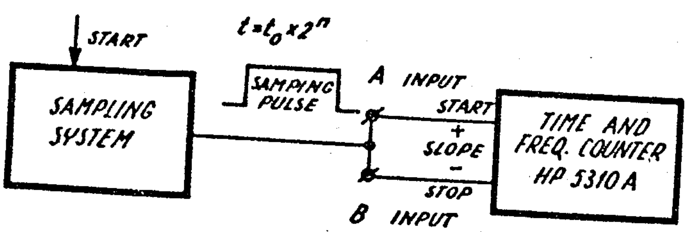

Fig. 6.4 Simplified block diagram for sampling time measurement

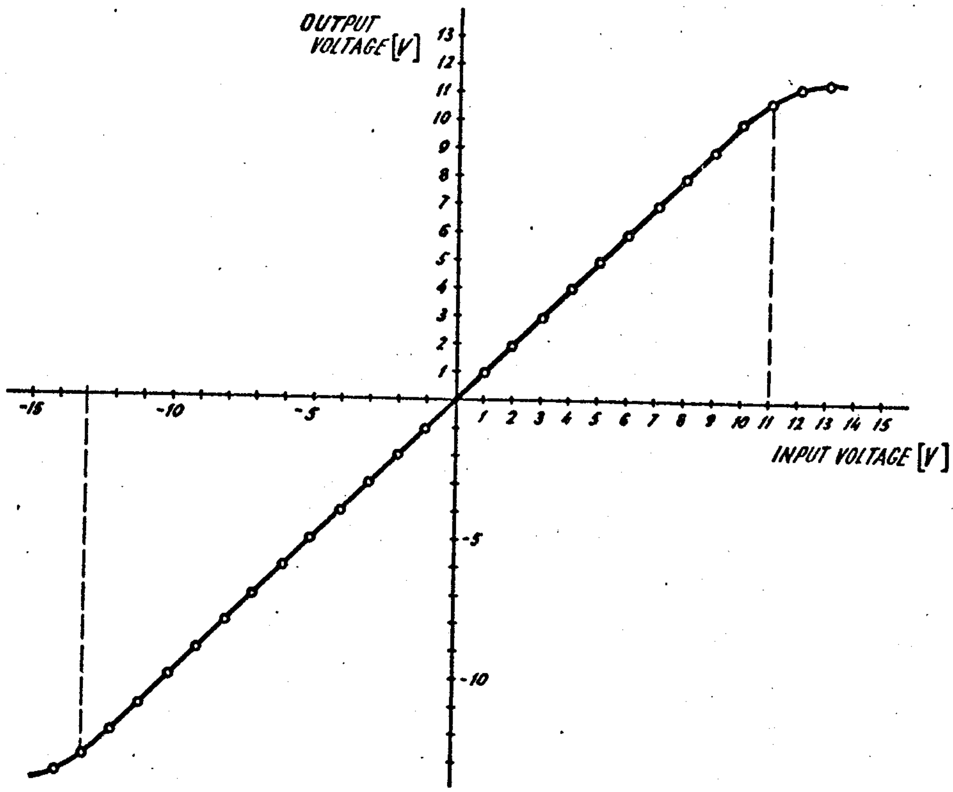

Fig. 6.5 Input-output characteristic of sampling system

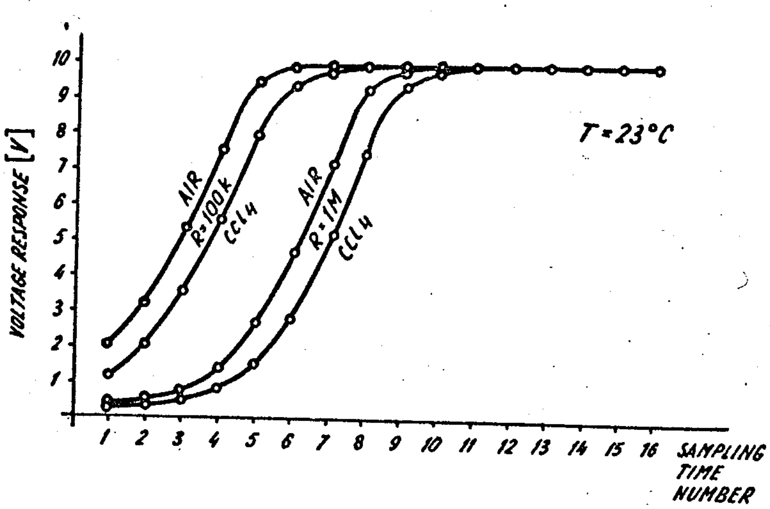

Fig. 6.6 Experimental results for Carbon tetrachloride - CCl_4

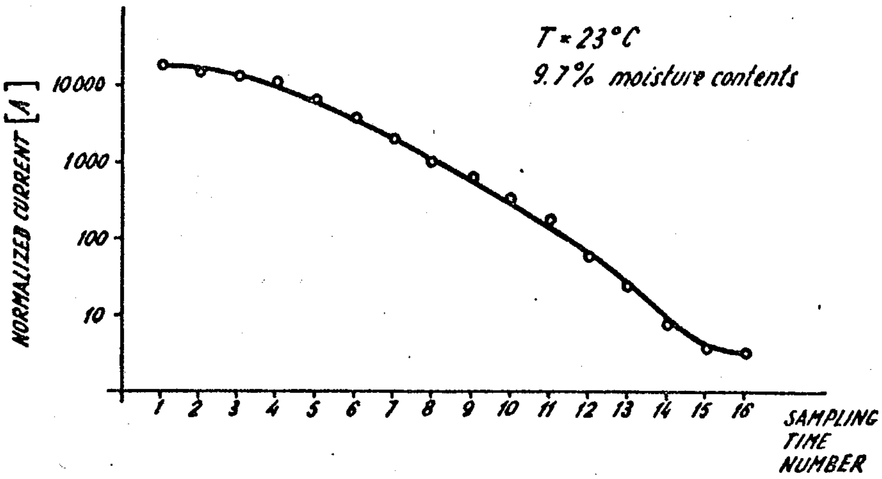

Fig. 6.7 Normalized current response for sample of wheat at 9.7% moisture contents and 23° C.

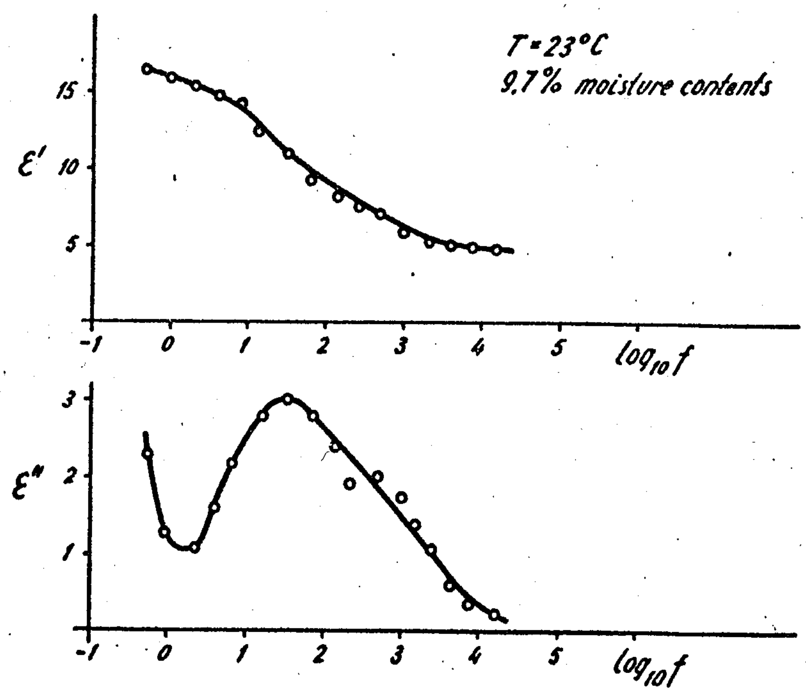

Fig. 6.8 Dielectric properties of sample of wheat at 9.7% moisture contents and 23° C.

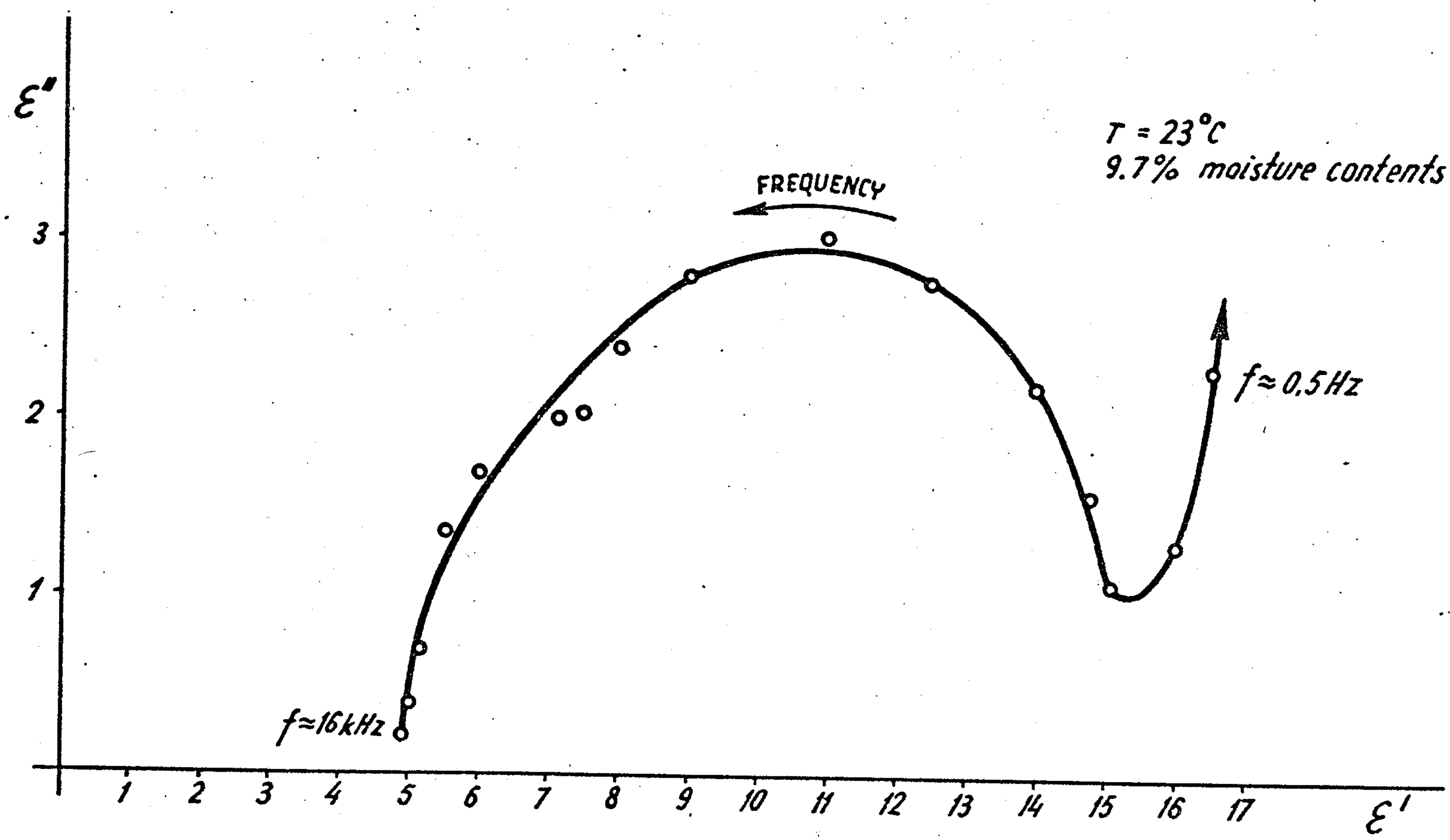

Fig. 6.9 Experimental results for sample of wheat at 9.7% moisture contents and 23° C.

Table 6.1 Experimental results for standard values of time constant. V_s = 10V

Sampling time [μs]	RC = 148.7 μs		RC = 1.03 ms		RC = 9.38 ms	
	Computed [mV]	Measured [mV]	Computed [mV]	Measured [mV]	Computed [mV]	Mesured [mV]
10	650	636	97	96	11	11
20	1 258	1 232	192	192	21	21
40	2 359	2 306	381	383	43	43
80	4 161	4 062	747	748	85	85
160	6 590	6 416	1 439	1 432	169	168
320	8 837	8 674	2 671	2 658	335	335
640	9 865	9 781	4 628	4 610	660	656
1 280	9 998	9 969	7 114	7 080	1 276	1 266
2 560	10 000	9 986	9 167	9 157	2 389	2 369
5 120	10 000	9 995	9 931	9 927	4 207	4 180
10 240	10 000	10 003	10 000	10 005	6 644	6 609
20 480	10 000	10 009	10 000	10 012	8 874	8 872
40 960	10 000	10 013	10 000	10 017	9 873	9 888
81 920	10 000	10 017	10 000	10 020	9 998	10 002
163 840	10 000	10 020	10 000	10 022	10 000	10 027
327 680	10 000	10 022	10 000	10 023	10 000	10 031

Table 6.2 Normalized current response for sample of wheat

Sampling time number	Sampling time [μs]	Voltage drop across R [mV]	Resistance R [kohm]	Charging current i/t/ [nA]	Normalized current C/N/ [A]
1	10	376	47	7798	18.180
2	20	796	100	7960	18.100
3	40	1195	200	5997	13.630
4	80	1754	390	4497	10.220
5	160	2868	820	3498	7.950
6	320	3445	1.500	2297	5.220
7	640	3049	3.300	924	2.100
8	1.280	2513	5.600	449	1.020
9	2.560	3696	10.000	370	840
10	5.120	3784	20.000	189	430
11	10.240	2244	30.000	75	170
12	20.480	714	30.000	24	54
13	40.960	320	40.000	8	18,2
14	81.920	160	40.000	4	9,1
15	163.840	100	50.000	2	4,5
16	327.680	100	50.000	2	4,5

$T = 23^{\circ}$ C

Moisture contents = 9.7%

Table 6.3 Experimental results for sample of wheat at 9.7% moisture contents and 23° C.

Frequency [Hz]	Real permittivity ε'	Loss factor ε''
15915.97	4.98	0.28
7957.98	5.00	0.49
3979.00	5.10	0.62
1989.50	5.36	1.05
994.75	6.00	1.77
497.37	7.07	2.08
248.69	7.95	1.92
124.34	8.64	2.39
62.17	9.91	2.91
31.09	11.58	3.12
15.54	13.15	2.88
7.77	14.28	2.17
3.89	14.99	1.60
1.94	15.44	1.07
0.97	15.77	1.36
0.49	16.61	2.27

CHAPTER 7

CONCLUSIONS

A technique for measurement of the complex permittivity has been investigated.

The background material, including basic parameters describing dielectric and their frequency dependance, have been presented.

The principles of both the frequency domain and time domain methods of measurements of the dielectric properties have been described.

The time domain measurement, based on the transient method, has been found most convenient for fast permittivity measurement over a wide frequency range.

An experimental system, including the sampling system and sample-holder capacitor, has been designed and developed to perform the measurement in time domain.

A computer program based on time to frequency domain transformation has been developed for finding the complex permittivity of the test material. The complex permittivity is calculated at sixteen discrete frequencies, spaced at octave intervals from 0.5 Hz to 16 kHz. The time taken to describe the complete spectrum is approximately 30 sec. The results are printed out versus logarithm of frequency, which is commonly used representation for dielectric properties.

The experimental system /hardware and software/ has been throughly tested, found satisfactory for dielectric measurements, and very simple in operation.

One disadvantage of the system is that it generates a discrete form of the results; however, this doesn't create any problems of interpretation.

Another problem creates a very large dynamic range of the recorded data, which strongly depends on the test dielectric. This requires one to set a proper value of small standard resistance in series with the sample-holder capacitor. For a lossy dielectric it is easy to do so, but many materials may require a few standard resistors to perform the measurement. This is a serious drawback of the method in fully automated systems.

A different type of double sample-holder capacitor with the guard electrode can substantially reduce the dynamic range of charging current. In this case it is possible to back off the part of the response current caused by geometric capacitance of the sample-holder.

The use of the linearly rising voltage, instead of step voltage, can be also a solution to this problem.

In order to develop fully automated systems suitable for the measurement of many different materials, the proposed system requires further study.

REFERENCES

1/ Von Hippel, A.R., Dielectric Materials and Applications, J.Wiley, New York, 1954.

2/ Hill, N.E., Vaughan, W.E., Price, A.H. and Davies, M., Dielectric Properties and Molecular Behaviour, Van Nostrand Reinhold Company, London 1969.

3/ Hyde, P.J., "Wide Frequency-range Dielectric Spectrometer", Proc. IEE, Vol 117, No. 9, September 1970, pp. 1891.

4/ Hamon, B.V., "An Approximate Method for Deducing Dielectric Loss Factor from Direct Current Measurements", Proc. IEE, part IV, Monograph No. 27, 1952.

5/ Davison, D.W., Auty, R.P. and Cole, R.H., "A Transient Method for Measurement of Dielectric Polarization", The Review of Scientific Instruments, Vol. 22, No. 9, 1951, pp. 678.

6/ Barid, M.E., "Determination of Dielectric Behaviour at Low Frequencies from Measurements of Anomalous Charging and Discharging Currents", Review of Modern Physics, Vol. 40, No. 1, January 1968.

7/ Field, R.F., Dielectric Materials and Applications, MIT Press, Cambridge, Mass., 1954.

8/ Stetson, L.E. and Nelson, S.O., "Audiofrequency Dielectric Properties of Grain and Seed", Trans. of the ASAE, Vol. 15, No. 1, 1972, pp. 180.

9/ Corcoran, P.T., Nelson, S.O., Stetson, L.E. and Schilaphoff, C.W., "Determining Dielectric Properties of

Grain and Seed in the Audiofrequency Range", Trans. of the ASAE, Vol. 13, No. 3, 1970, pp. 348.

10/ Nelson, S.O., "Electrical Properties of Agricultural Products. A Review", for presentation at the 1971 Winter Meeting American Society of Agricultural Engineers, Chicago, Illinois, December 1971.

11/ Iskander, M.F. and Stuchly, S.S., "A Time Domain Technique for Measurements of the Dielectric Properties of Biological Substances", IEEE Trans. Instrum. Meas., Vol. IM-21, No. 1, pp. 56-62, 1974.

12/ Böttcher, C.J.F., Theory of Electric Polarization, Elsevier Publishing Company, 1952.

13/ Van Gemert, M.J.C., "High-Frequency Time - Domain Methods in Dielectric Spectroscopy", Philips Res. Repts 28, pp. 530-572, 1973.

14/ Hoeschele, D.F.Jr., Analog to Digital/ Digital to Analog Conversion Techniques, J.Wiley, New York, 1968.

15/ Schmid, H., Electronic Analog/Digital Conversions, Van Nostrand Reinhold Company, New York, 1970.

APPENDIX I

SCHEMATIC DIAGRAMS

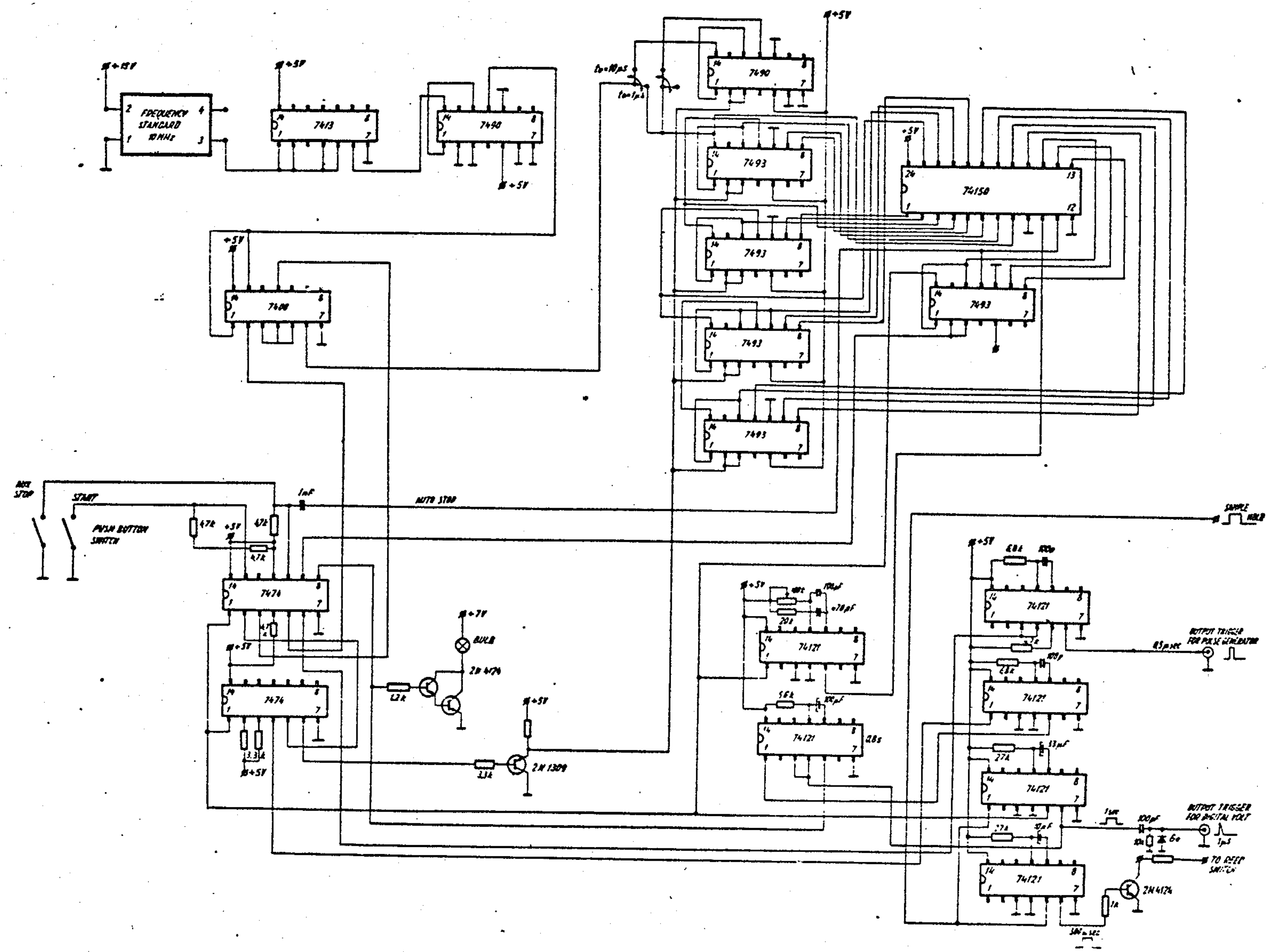

Fig. A.1 Schematic diagram of the Control Circuit

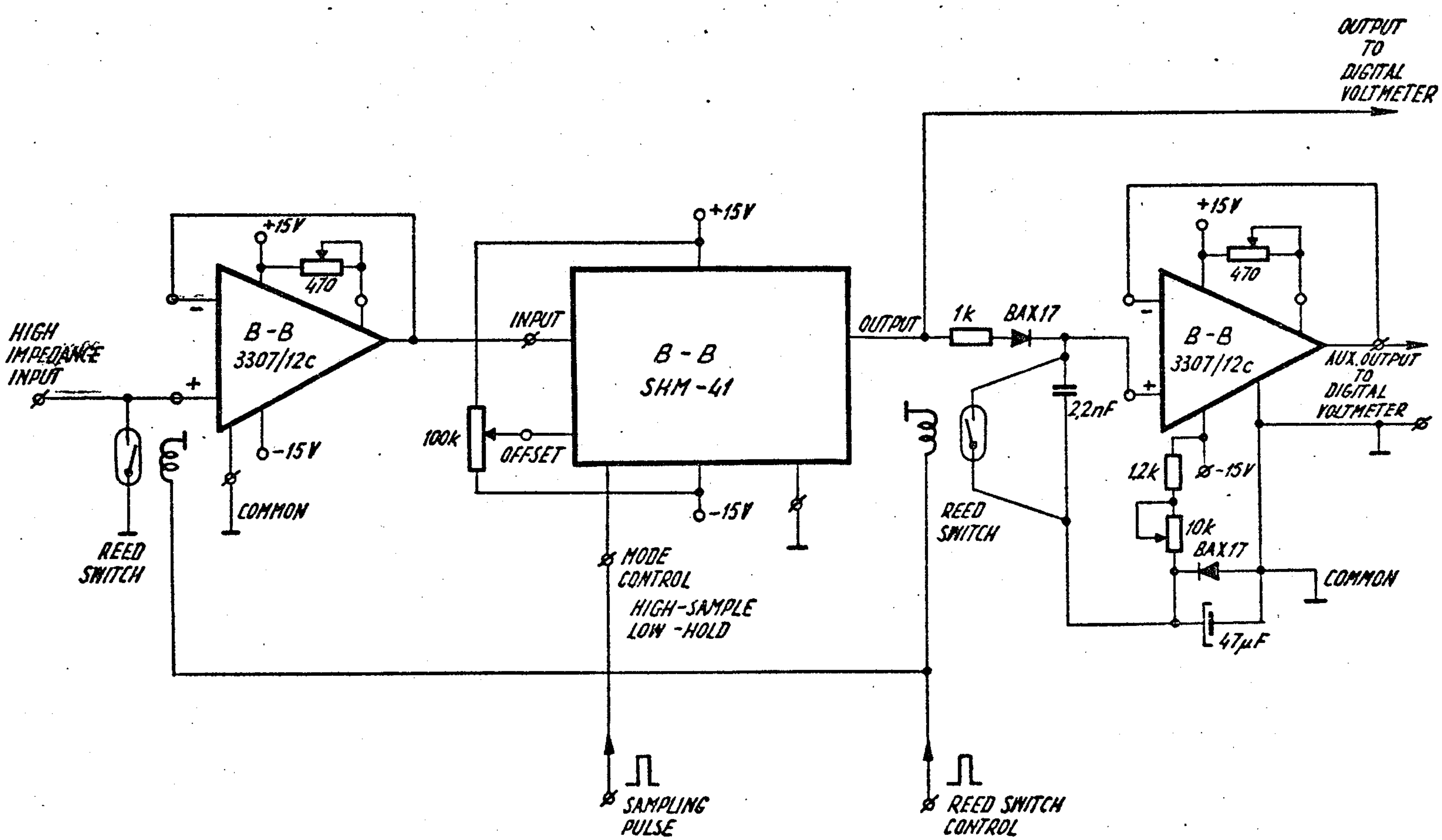

Fig. A.2 Schematic diagram of the Input Circuit

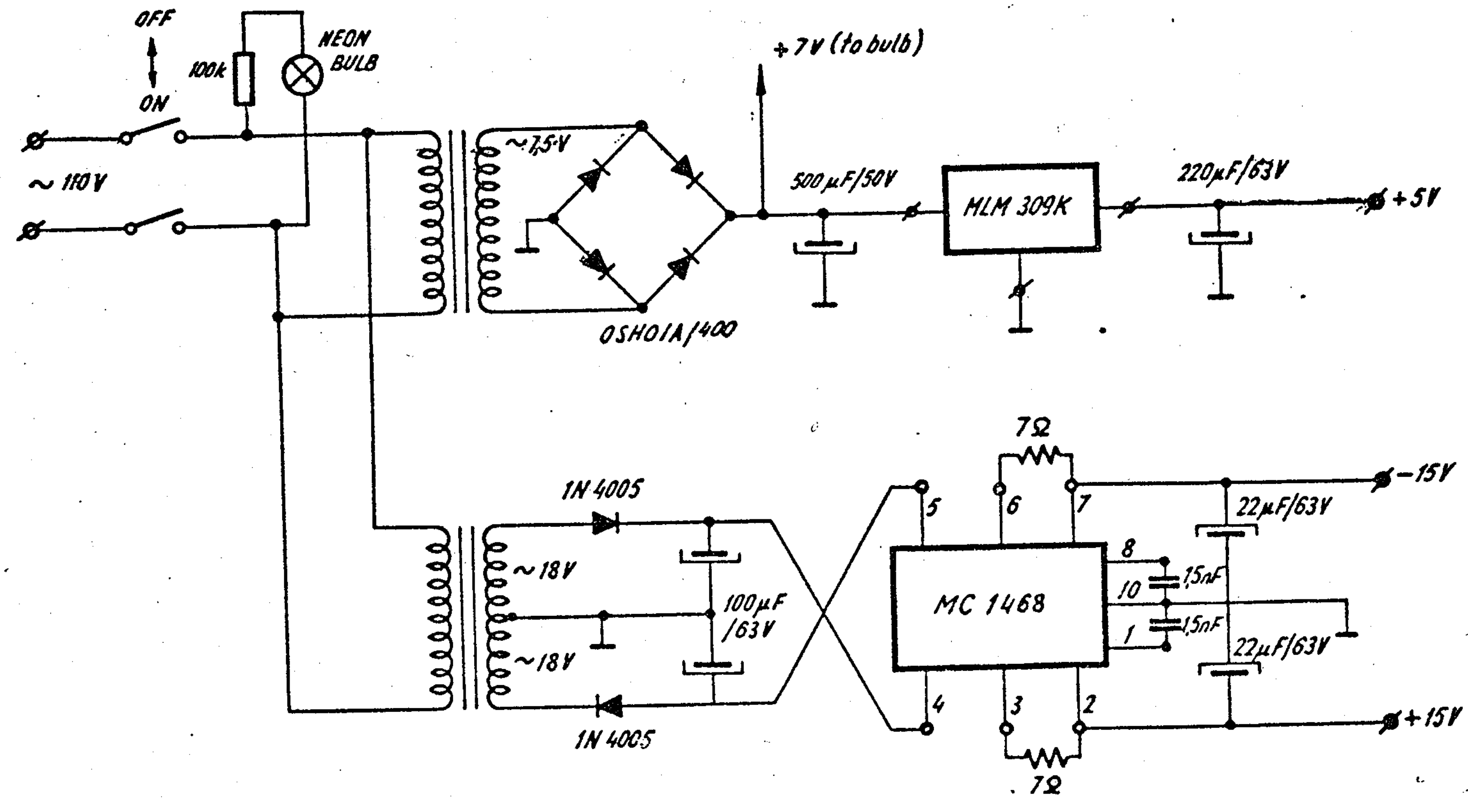

Fig. A.3 Schematic diagram of the power supply

APPENDIX 2

COMPUTER PROGRAM

A computer program was developed to compute the values of the complex permittivity as a function of frequency.

Calculations were programmed for computation on an IBM 360/65 computer using FORTRAN IV programming language.

```
$JOB WATFIV      WITOLD MATULEWICZ
C COMPUTER PROGRAM FOR TIME TO
C FREQUENCY DOMAIN TRANSFORMATION
      DIMENSION C(128)
      DIMENSION DQ(128)
      DIMENSION A(129)
C EVALUATION OF COEFFICIENTS
      DIMENSION X(11),Y(11)
      READ,(X(I),I=1,11)
      READ,(Y(I),I=1,11)
      SUM1=0
      DO 1 I=1,4
    1 SUM1=SUM1+Y(I)
      SUM2=0
      SUM3=0
      DO 2 I=8,11
      SUM2=SUM2+X(I)
    2 SUM3=SUM3+Y(I)
C DATA READING
C M-NUMBER OF SAMPLES
C TC-INITIAL SAMPLING TIME
C C(N)-DATA,CURRENT THROUGH SPECIMEN
      READ,M
      READ,TC
      READ,(C(N),N=1,M)
      PRINT5
    5 FORMAT('-','DATA')
      PRINT6,(C(N),N=1,M)
    6 FORMAT('0'16F8.1)
C DQ(N)-INCREASE OF TIME INTEGRAL OF
C CURRENT THROUGH SPECIMEN
C T-TIME
      T=TC
      DO 3 N=1,M
      DQ(N)=C(N)*T*ALOG(2.)
    3 T=T*2
      PRINT,(DQ(N),N=1,M)
C A(N)-TIME INTEGRAL OF CURRENT THROUGH SPECIMEN
C A(1)-TOTAL CHARGE TRANSFERED FROM
C TIME T=0 UP TO T=TC/SQRT(2)
      READ,A(1)
      L=M+1
      DO 4 N=2,L
    4 A(N)=A(N-1)+DQ(N-1)
      PRINT,(A(N),N=1,M)
C COMPUTATION OF COMPLEX PERMITTIVITY VERSUS FREQUENCY
C E1-REAL PART OF COMPLEX PERMITTIVITY
C E2-IMAGINARY PART OF COMPLEX PERMITTIVITY
C F-FREQUENCY
```

```
          PRINT50
    50    FORMAT('1',9X,'F',11X,'E1',10X,'E2')
          T=TO
          DO 10 N=1,M
          F=1/(T*2*3.1415)
          IF(T.LT.2*TO) GO TO 20
          IF(T.LT.3*TO) GO TO 30
          IF(T.GT.TO*2**14) GO TO 20
          IF(T.GT.TO*2**13) GO TO 30
          E1=A(N-2)+
         XX(4)*(A(N-1)-A(N-2))+
         XX(5)*(A(N)-A(N-1))+
         XX(6)*(A(N+1)-A(N))+
         XX(7)*(A(N+2)-A(N+1))+
         XSUM2*(A(N+3)-A(N+2))

          E2=SUM1*(A(N-1)-A(N-2))+
         XY(5)*(A(N)-A(N-1))+
         XY(6)*(A(N+1)-A(N))+
         XY(7)*(A(N+2)-A(N+1))+
         XSUM3*(A(N+3)-A(N+2))
          GO TO 40
    30    E1=A(N-1)+
         XX(5)*(A(N)-A(N-1))+
         XX(6)*(A(N+1)-A(N))+
         X(X(7)+SUM2)*(A(N+2)-A(N+1))
          E2=(SUM1+Y(5))*(A(N)-A(N-1))+
         XY(6)*(A(N+1)-A(N))+
         X(Y(7)+SUM3)*(A(N+2)-A(N+1))
          GO TO 40
    20    E1=A(N)+(X(6)+X(7)+SUM2)*(A(N+1)-A(N))
          E2=(SUM1+Y(5)+Y(6)+Y(7)+SUM3)*(A(N+1)-A(N))
    40    T=T*2
          PRINT51,F,E1,E2
    51    FORMAT('-',3F12.2)
    10    CONTINUE
          STOP
          END

$ENTRY
```